Removal of Organic Films from Rotating Disks Using Aqueous Solutions of Nonionic Surfactants: Film Morphology and Cleaning Mechanisms

J. A. Kabin, A. E. Sáez, C. S. Grant, and R. G. Carbonell*

Department of Chemical Engineering, North Carolina State University, Box 7905, Raleigh, North Carolina 27695-7905

In this work, we consider the cleaning of an organic liquid film, consisting initially of a concentrated solution of abietic acid in isopropyl alcohol, from the surface of a rotating disk by using aqueous solutions of a nonionic surfactant, pentaethylene glycol mono-*n*-dodecyl ether. The results show that the removal process takes place in three consecutive stages. The first stage is controlled by the solubilization of the abietic acid by surfactant penetration and subsequent mass transfer from the interface to the bulk of the aqueous solution. During the first stage, the film absorbs water from the aqueous solution and breaks up into drops that leave portions of the surface exposed. The absorption of surfactant and water reduces the organic-phase viscosity, until the drops start to move on the disk surface under the action of shear forces. These drops aggregate into spiral-shaped continuous rivulets through which the organic phase flows until it comes off the disk edge. Such behavior occurs during the second stage of cleaning, which has a rate of removal appreciably faster than the first stage. The rivulets are shown to be tangent to the stress exerted by the aqueous solution on the surface of the organic phase. The rivulets eventually break, leading to a third stage with lower removal rates, in which the removal mechanism is apparently the roll up of organic-phase drops under the action of shear forces. In this work, we present experimental evidence that supports the described mechanism, based on photographs showing the morphology of the film structure in the different cleaning stages. A model is derived that relates the empirical observations of cleaning rates to physical parameters describing the solubilizing film hydrodynamics.

Introduction

The removal of organic films from solid substrates is an important step in industrial manufacturing processes such as the fabrication of circuit boards. In this process, flux residues are removed by using cleaning solutions whose formulations contain CFC-113 or other alternative solvents. Flux is a product employed to clean metallic leads of printed wiring assemblies and electronic components before soldering. Traditional flux formulations contain abietic acid as their main component solubilized in a carrier liquid (typically isopropyl alcohol). In previous works (Beaudoin et al., 1995a,b) we have shown how aqueous solutions of nonionic surfactants can accomplish the removal of abietic acid films from laminate substrates, a process that represents a viable alternative to the use of chlorofluorocarbons.

It is widely accepted in the literature that the cleaning of oily residues from surfaces by surfactant solutions proceeds according to one of three different mechanisms: solubilization, emulsification, and roll-up (Rosen, 1989; Miller and Raney, 1993). In solubilization, the organic phase is incorporated into micelles that desorb from the oil surface into the aqueous solution. Emulsification involves the formation of a microemulsion of oil in water in the vicinity of the oil−water interface which is then removed into the aqueous phase by either hydrodynamic forces or diffusion. Finally, roll-up designates a mechanism in which the adsorption of surfactant significantly reduces the contact angle of the aqueous solution on the substrate at the water−substrate−oil contact line, leading to the formation of organic-phase drops that are then removed from the surface by mechanical forces.

The rotating disk apparatus is a device that has been used to study the removal of organic films from solid surfaces (Beaudoin et al., 1995a,b). A thin film of the organic liquid is deposited on the disk surface, and then the disk is immersed into the cleaning solution and rotated at a constant angular speed. The rotating disk system is relatively simple from an experimental standpoint, and its hydrodynamics and mass transfer are well characterized in the literature. Previous works have identified cleaning kinetics that are linear in terms of moles of organic component removed as a function of time. For example, Shaeiwitz et al. (1981) quantified this linear kinetics in terms of a solubilization mechanism whose controlling step was the mass transfer of micelles containing the organic component from the oil−water interface to the bulk of the aqueous solution.

In our previous works, a more complex cleaning mechanism was found in the removal of abietic acid films from epoxy−glass laminate surfaces. Beaudoin et al. (1995a) observed that the cleaning process consisted of three stages. A typical cleaning curve is shown in Figure 1. In this figure, N_A represents the total moles of abietic acid removed from the disk at a given time t. At early times, a linear cleaning rate was found, in which abietic acid removal was relatively slow (stage 1). At a specific onset time, denoted by t_c, the cleaning rate increased abruptly, leading to stage 2, in which typically most of the abietic acid removal took place. Finally, the cleaning rate substantially decreased (stage 3) and complete removal of the organic film occurred asymptotically with time. The transition from stage 2

* To whom correspondence should be addressed. E-mail: ruben@ncsu.edu. Phone: (919) 515-2499. Fax: (919) 515-3465.

S0888-5885(96)00195-9 CCC: $12.00 © 1996 American Chemical Society

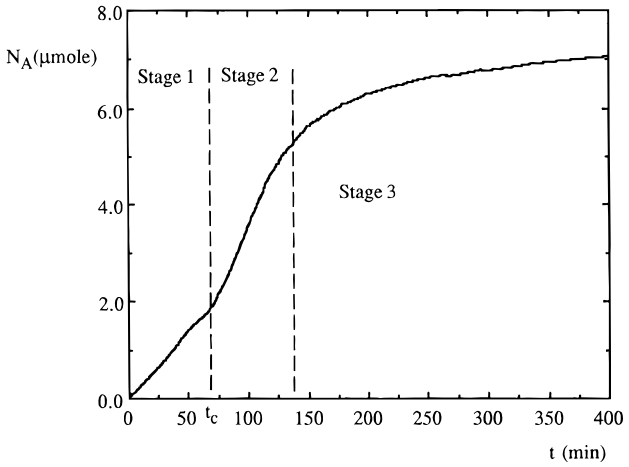

Figure 1. Typical cleaning curve of an abietic acid film from a rotating disk. The cleaning solution is an aqueous solution of $C_{12}E_5$ with a concentration of 6×10^{-5} M. The rotational speed of the disk is 1750 rpm.

to stage 3 is more gradual than the rate increase observed at the beginning of the second stage.

Beaudoin et al. (1995b) proposed a model to explain the three consecutive cleaning stages. In that work, we suggested that during stage 1, the surfactant penetrated the organic film, causing it to absorb water, which set the appropriate conditions for stage 2, in which abietic acid droplets were removed from the surface by the action of shear forces exerted on the film by the moving aqueous solution. After a certain amount of the original abietic acid was removed, part of the substrate was exposed to the aqueous solution, thus reducing the cleaning rate and leading to stage 3. The cleaning process in stage 3 was also found to be controlled by hydrodynamic forces. The main evidence that supported the analysis was that cleaning rates during stages 2 and 3 were directly proportional to $\omega^{3/2}$, which is precisely the scaling between average shear stress at the surface and angular velocity. Beaudoin et al. (1995a) analyzed the effect of surfactant concentration and rotational speed on the cleaning rates during stages 2 and 3.

In this work, we explore in more detail the cleaning mechanisms governing the removal of organic films from rotating disks. This is accomplished by performing a photographic study of the film morphology as cleaning proceeds through the three stages. The main objective of this work is to establish the physics of the cleaning process and propose theoretical models that simulate the process by taking into account the basic mechanisms and the film morphology in the various cleaning stages.

Experimental Section

A detailed description of the experimental apparatus, materials, and measuring techniques is given elsewhere (Beaudoin et al., 1995a). Here we will present a brief summary of the experimental aspects of the work.

The disks used in the experiments were cut from flat sheets of FR-4 fiberglass laminate provided by Northern Telecom. This material consists of layers of glass fabric epoxied together using brominated epoxy resins (Beaudoin et al., 1995a). They were 2.1 cm in diameter. The disks were spin coated with one application of a 42% by weight solution of abietic acid in isopropyl alcohol. After the coating process, the disks were placed in a dessicator at room temperature for 24 h and then stored in a refrigerator. It was determined that the film of abietic acid solution on the disk had an initial thickness of approximately 10 μm (Beaudoin et al., 1995a), and it consisted of an approximately 75% by weight solution of abietic acid in isopropyl alcohol. The change in abietic acid content is due to alcohol evaporation during spin coating and storage. It is important to point out that the abietic acid is a solid at the conditions of the experiments. The final film on the disks, which contains 25% by weight isopropyl alcohol, is a viscous liquid. As will be shown in the following section, the organic phase on the disk always appears to be in liquid form. The absorption of surfactant and water by the abietic acid contributes to keep the film in liquid form. On the basis of this observation, we will concentrate on the removal of abietic acid from the disk, neglecting the effects of the isopropyl alcohol in the process.

The coated disks were press-fit into a Teflon holder so that they were flush with the Teflon surface, forming a structure with a total diameter of 4 cm. The disk holder was coupled to a shaft, leading to a precision rotator. Rotational speeds ranging from 250 to 1750 rpm were used in the experiments.

The disks were spun in a reservoir containing 500 cm^3 aqueous solutions of the nonionic surfactant pentaethylene glycol mono-*n*-dodecyl ether ($C_{12}E_5$), provided in monodisperse form by Nikkol Chemicals. The surfactant solutions ranged in concentrations from 6×10^{-5} to 4.1×10^{-3} M. The lowest concentration employed (6×10^{-5} M) was slightly below the cmc of the aqueous solution (6.4×10^{-5} M). All the experiments were performed at 24 °C.

Quantities of the abietic acid removed from the disk were measured by passing part of the surfactant solution through a UV detector at a flow rate of 10 cm^3/min. The detection was performed at a wavelength of 254 nm. The residence time of the solution in the UV detector loop is approximately 1 min, which is appreciably lower than the characteristic times of the cleaning experiments. In this way, an instantaneous measure of abietic acid concentration in the aqueous solution was obtained as a function of time. This allowed calculation of the moles of abietic acid removed from the surface as a function of time.

The concentration of abietic acid in the aqueous solution (500-cm^3 reservoir) was at the end of the experiment of the order of 10^{-5} M. Such low levels ensured that the dissolved abietic acid did not interfere with the kinetics of the cleaning process.

The evolution of the film morphology during the cleaning process was studied by taking photographs of the disk surface at various cleaning times. In this type of experiment, the cleaning was continuously monitored until it reached a desired point in the cleaning curve. At this time, rotation was stopped, the disk was removed from the apparatus, and the remaining water on it was allowed to run off. The disk was then photographed using a reflective microscope (Reichert MeF2 Metalograph) at a 12X magnification and later discarded.

Cleaning Mechanisms and Film Morphology

In this section, we analyze the cleaning mechanisms and the evolution of film morphology during the cleaning process, as revealed by photographs of the film taken at the different cleaning stages. As a basis for this analysis, we have selected as a representative case an

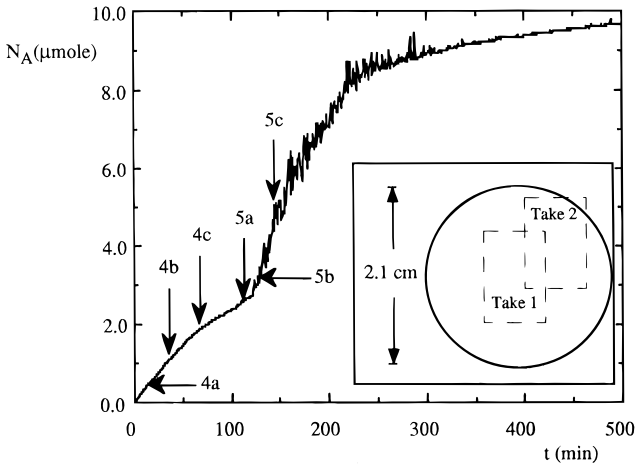

Figure 2. Cleaning curve for the film morphologies presented in Figures 4 and 5; $\omega = 750$ rpm; $C_s = 6 \times 10^{-5}$ M. The inset shows a sketch of the disk areas covered by the photographs.

experiment with a surfactant concentration of 6×10^{-5} M and a rotational speed of 750 rpm. This case was selected because it encompasses all the film morphologies observed during the course of this work. The cleaning curve for this case is presented in Figure 2. This figure also shows the relative location on the disk of the areas covered by the two different types of photograph taken: one includes the disk center (take 1), and the other one covers the region close to the edge (take 2). The arrows on the curve show the approximate location in the cleaning process at which the photographs presented in Figures 4 and 5 were taken.

As will be discussed in the next section, the first stage of the cleaning process consists of a solubilization mechanism controlled by the desorption of the abietic acid from the film surface and its transport into the bulk surfactant solution. In order to gain insights into this process, we performed an experiment in which cleaning was allowed to take place under static conditions. In this experiment, the disk was immersed in a 1×10^{-3} M surfactant solution without rotation. Figure 3 shows a sequence of photographs of the disk surface as time passes. In this and subsequent photographs, the organic phase (film) appears light, whereas the exposed surface of the laminate disk appears dark. It should be recalled that each photograph corresponds to a stopped experiment on a different disk. Figure 3a shows the original film on the disk, before immersing it into the surfactant solution. This photograph is typical of the disks employed in all the experiments. It is clear that the film does not have a uniform thickness but that it is essentially rough. Some of the depressions of the film seem to go down to the substrate surface, leaving a small fraction of the laminate surface exposed. The lack of uniformity of the original film can be attributed to two factors: first, since the laminate surface is rough, the spin-coating process, which is carried at high rotational speeds (2000 rpm), might lead to the development of ripples on the film surface due to flow instabilities, such as those observed in film flow experiments over rotating disks performed by Thomas et al. (1991). Second, the evaporation of isopropyl alcohol during and after the spin coating contributes to the formation of holes and cracks on the film surface.

As time passes, the original depressions on the film are enlarged and new ones are formed as the abietic acid is removed from the disk by solubilization into the surfactant solution. After enough time has elapsed, the

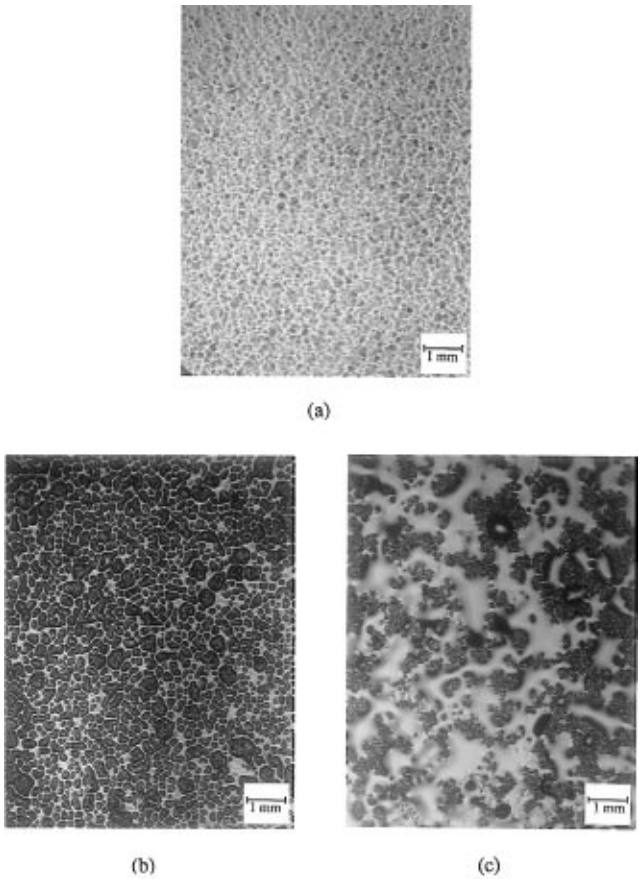

Figure 3. Film morphology during cleaning process without disk rotation. Photographs correspond to take 1; $C_s = 1 \times 10^{-3}$ M. (a) Before cleaning. (b) $t = 4$ h. (c) $t = 44$ h.

distribution of organic phase on the surface resembles a two-dimensional honeycomb structure (Figure 3b) which exhibits relatively large holes of exposed laminate surface and thin strands of organic film surrounding them. This particular morphology is caused by the progressive reduction in film thickness as the abietic acid is dissolved, and it is affected by the irregularities of the initial film surface. At the point shown in Figure 3b, around 10% of the abietic acid has been removed from the disk. At longer times, Figure 3c, the thread-like organic films are replaced by larger structures that coalesce, leading to a pattern in which relatively large drops of organic phase exist on the disk surface. This is caused by the penetration of a sizable amount of water into the organic film, leading to its liquefaction. The absorption of water into the film is caused by the partitioning of surfactant into the organic phase and the solubilization of the water into the resulting organic phase. This phenomenon was previously detected in static partitioning experiments (Beaudoin et al., 1995a). For the condition reported in Figure 3c, between 30% and 40% of the abietic acid has been removed from the disk. Notice that, judging from the surface coverage of the film, a comparison between parts b and c of Figure 3 indicates that there has not been a large reduction in film volume, even though a sizable amount of abietic acid has been removed in the time between the two photographs. This confirms the swelling of the film by water solubilization in that period. It is interesting to point out that there is no water partitioning into the organic phase in the absence of surfactant; i.e., water is essentially insoluble in the organic phase. This means that the water that parti-

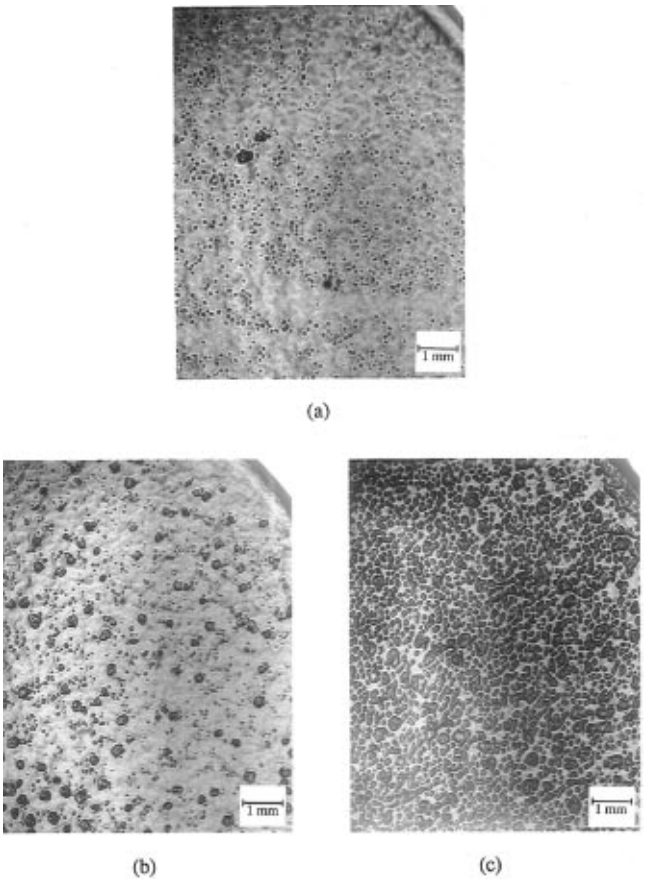

Figure 4. Film morphology during stage 1. Photographs correspond to take 2. Time of photographs reported in Figure 2.

tions into the film either is contained in surfactant reverse micelles or is forming a microemulsion within the film.

The morphology of the films was also studied in the cleaning experiments. It was found that film morphology was qualitatively different in each of the three stages of cleaning. In fact, the film morphology provides evidence of the basic mechanisms that control the evolution of the cleaning process, as is discussed below.

Figure 4 shows film morphology as a function of time during stage 1 of a cleaning experiment with a rotational speed of 750 rpm and a surfactant concentration of 6×10^{-5} M (for the location of each stage in the cleaning curve, see Figure 2). In Figure 4a, the original depressions of the film begin to enlarge and small holes begin to form. Notice that the spatial distribution of the holes seems to be macroscopically uniform over the whole surface of the disk. For longer times (Figure 4b), the holes continue to enlarge and new ones are formed, until a honeycomb structure is reached (Figure 4c). This last photograph is well into, but close to the end of, stage 1, as shown in Figure 2.

The process presented in Figure 4 resembles the first part of the diffusion experiment (Figure 3a and b). This observation leads us to conclude that the first stage of the dynamic cleaning process is governed by the solubilization of the organic film into the surfactant solution. The main apparent difference between Figures 3 and 4 is the time that it takes to reach each of the morphologies. Note that for the conditions in Figure 4c, less than 20% of the original abietic acid has been removed (Figure 2). It is interesting to point out that hydrodynamic forces do not seem to be playing a role in the cleaning process during stage 1 because the shear stress acting on the film is a linear function of radial position, starting from zero at the center (Beaudoin et al., 1995b). If a roll-up mechanism were responsible for cleaning in stage 1, one would expect to see a variation in the cleaning pattern with radial position, a feature that is not observed in Figure 4. On the other hand, for a rotating disk apparatus, mass-transfer rates are radially uniform (Levich, 1942), which is consistent with the observations.

As the first stage proceeds to its end, the film of organic phase on the surface starts to swell with surfactant and water, as in the diffusion experiment (Figure 3c). The swollen organic phase becomes progressively less viscous until it starts to flow on the surface under the action of the shear stress exerted by the motion of the aqueous phase. This is seen in Figure 5, which shows the change in morphology of the organic phase as the cleaning process goes into stage 2. In Figure 5a, coalesced, swollen structures can be observed, similar to those in Figure 3c. Notice that, close to the edge of the disk in Figure 5a, the drops of organic phase on the surface tend to form coherent structures in the shape of spiral curves. These structures are rivulets of swollen organic phase that start at a given radial position and extend to the edge of the disk, through which the abietic acid flows and goes off the disk. We will show in the next section that the rivulets follow approximately the lines of constant shear stress on the disk so that their shape and formation is controlled by the hydrodynamic forces exerted by the aqueous solution on the organic phase.

As time passes, the morphology of the organic phase evolves into a pattern of rivulets that extends to a region close to the center of the disk (Figure 5b). Around the disk center, however, the rivulets are not present and the organic phase retains the shape of drops attached to the disk surface since the shear stress near the center is small and it apparently cannot induce a motion of the organic phase in that region. This analysis suggests that a necessary condition for the formation of the rivulets and the removal of abietic acid through the edges of the disk is the liquefaction of the abietic acid film, since its viscosity must be reduced before the shear stresses can make the organic phase flow on the surface. As time elapses, the rivulets start to disappear, reducing their number and breaking (Figure 5c).

The motion of the organic phase on the surface and its subsequent removal through the edges of the disk causes the increase in the cleaning rate observed at the beginning of stage 2 (see Figure 2). These observations are consistent with the analysis of Beaudoin et al. (1995b), who argued that the cleaning process in stage 2 was controlled by hydrodynamic forces that resulted in the detachment of organic-phase drops from the surface. Further evidence supporting this mechanism is the presence of spikes in the cleaning curves during stage 2, caused by the delay in the solubilization of the detached abietic acid drops as they pass through the UV detector. The observations made in this work serve to determine the precise effect of the hydrodynamic forces and to establish that the detachment of abietic acid drops occurs at the edge of the disk.

During stage 3, the film morphology follows the disappearance of the rivulets and the drops around the disk center, until the organic phase is completely removed from the disks. Photographs of this stage (not shown here) did not reveal any additional features. However, as will be discussed below, the removal of the

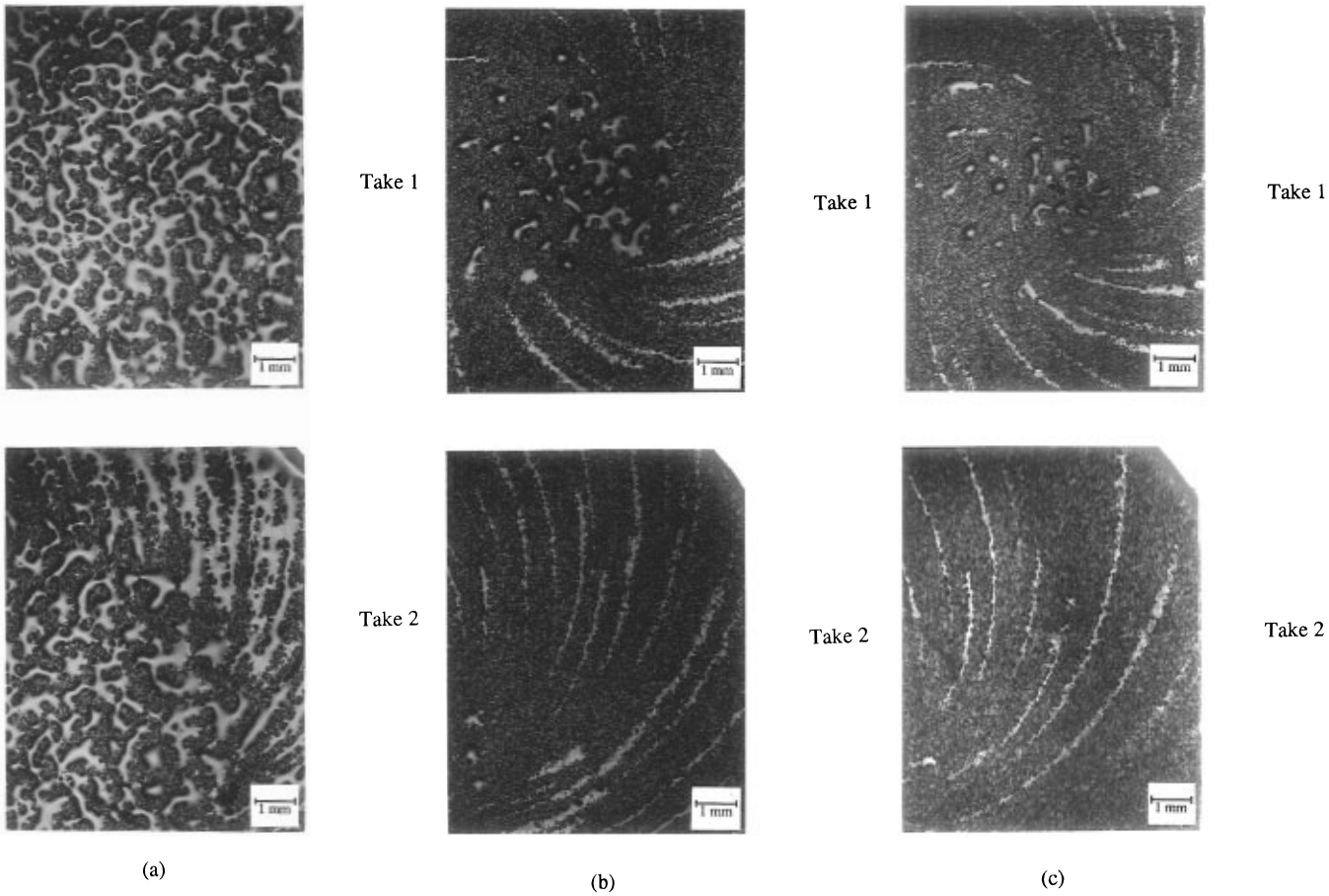

Figure 5. Film morphology evolution as the process goes into stage 2. Time of photographs reported in Figure 2.

organic film in this last stage seems to follow a roll-up process in which hydrodynamic forces play an important role. The reduction in cleaning rate as the system goes from stage 2 to stage 3 is caused by the breaking of the rivulets and the depletion of the organic film on the disk surface.

The formation of rivulets by the end of stage 1 involves the displacement and coalescence of organic-phase drops on the surface under the action of shear stresses. In this process, the interfacial and rheological properties of the swollen film droplets must play an important role. For a given system and surfactant concentration, the magnitude of hydrodynamic forces is controlled by the rotational speed. The effect of rotational speed on rivulet morphology is shown in Figure 6, where photographs of the transition between stages 1 and 2 are shown for the same surfactant concentration and different rotational speeds. These photographs show that the rivulets formed at low rotational speeds seem to be somewhat thicker and meander more on the surface than those formed at high rotational speeds. The most noticeable difference between parts a and b of Figure 6 is the extension of the rivulets to the central region of the disk at the high rotational speed (Figure 6b) due to the presence in this case of larger shear stresses in that region. At the low rotational speed (Figure 6a), the stresses close to the center of the disk are not enough to cause motion of the drops on the surface.

In the following section, a theoretical development is presented which complements the morphological observations performed above. Quantitative results regarding cleaning rates in the different cleaning stages are also demonstrated.

Theoretical Analysis of Cleaning Rates

Stage 1. The observations indicate that the first stage consists of a solubilization mechanism in which abietic acid is dissolved into the aqueous phase by the action of the surfactant. The process includes the following steps: (1) mass transfer of the surfactant from the bulk of the aqueous solution to the vicinity of the film surface; (2) absorption of surfactant onto the interface; (3) formation of micellar aggregates containing abietic acid molecules that desorb from the interface into the aqueous phase; (4) mass transfer of the micelles from the interface region to the bulk of the aqueous solution.

Furthermore, the surfactant is simultaneously being transported into the organic phase, and water from the aqueous solution is being solubilized into the organic phase.

Beaudoin et al. (1995a) observed that the cleaning curves were linear during the first stage, which indicates a constant rate of abietic acid removal from the film. This seems to be consistent with previous investigations where the amount of organic phase removed from the rotating disk changes linearly with time (see, for example, Shaeiwitz et al., 1981). In some of the experiments performed in this work, the first-stage cleaning curve was not a straight line (see Figure 2) but exhibited a slight reduction in its slope as time increased. Such a cleaning rate decrease is mainly a consequence of the reduction of the film surface as time progresses, as evidenced by Figure 4. The slight downward curvature occurred at low surfactant concentrations and low rotational speeds only.

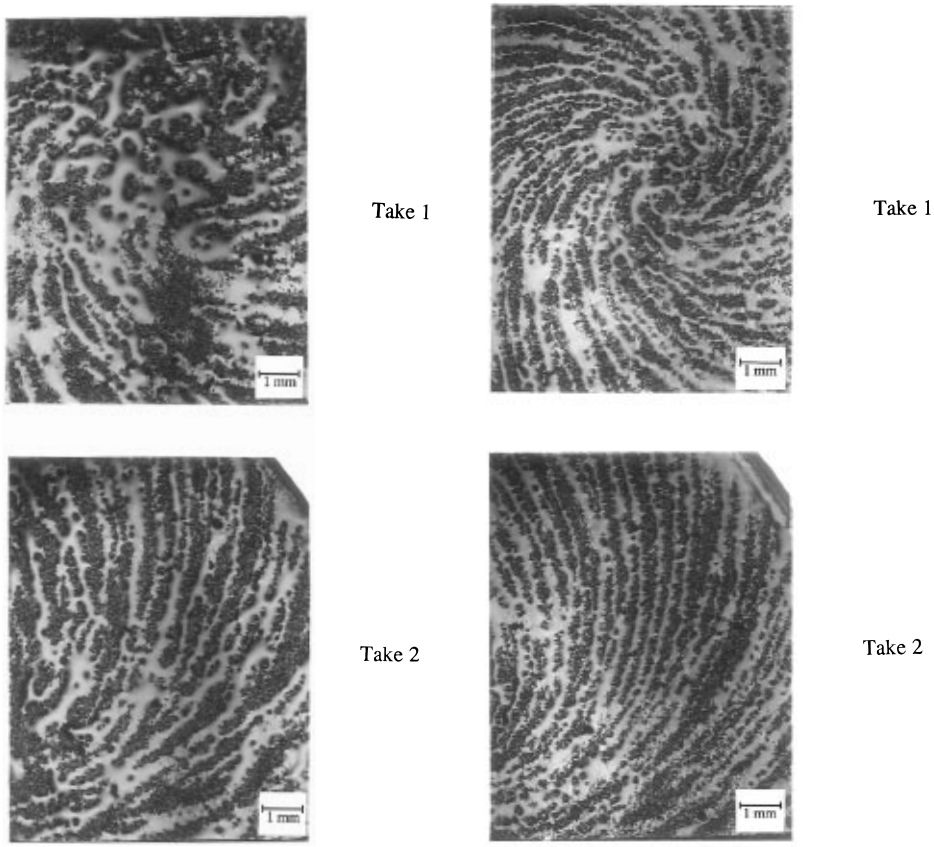

Figure 6. Film morphology in stage 2 for two different rotational speeds; $C_s = 1 \times 10^{-3}$ M. (a) $\omega = 250$ rpm. (b) $\omega = 1750$ rpm.

Our analysis of cleaning during stage 1 assumes that surfactant transport to the interface is fast compared to the rest of the steps in the mechanism. Additionally, the partitioning of surfactant into the organic phase is also assumed to be fast. This assumption can be verified by means of an order of magnitude analysis (see Appendix). Under these conditions, the concentration of adsorbed surfactant on the interface is constant throughout the first stage, and its value is dictated by equilibrium considerations. The concentration of surfactant in the aqueous phase at the interface is always equal to the bulk value (C_s).

Let r_R be the specific rate of desorption of abietic acid from the film surface into the aqueous solution (moles of acid removed per unit time and area). Given the assumption postulated above, this parameter is only a function of C_s and temperature. On the other hand, let r_A be the rate of adsorption of abietic acid from the aqueous solution onto the interface. A balence of abietic acid at the interface yields

$$\text{net rate of abietic acid removal} = k_A A(C_A^* - C_A) = A_a(r_R - r_A) \quad (1)$$

In this expression, k_A is the mass-transfer coefficient of abietic acid from the interface to the bulk of the aqueous phase, C_A and C_A^* are the concentrations of abietic acid in the bulk solution and at the interface, respectively, A is the disk surface area, and A_a is the exposed area of the film. In establishing eq 1, we have assumed that there is no abietic acid accumulation in the interface region and that the abietic acid concentration is radially uniform on the surface of the disk; i.e., the abietic acid solubilized from the film rapidly mixes radially. These assumptions will lose validity only when the organic phase is distributed in isolated drops on the surface. The assumptions are consistent with the classical analysis of mass transfer from a rotating disk (Levich, 1942).

It is interesting to point out that the abietic acid transported from the interface to the bulk solution is presumably contained in surfactant micelles so that the mass-transfer coefficient, k_A, reflects the transport of the micelles.

As the observations reported in the previous section revealed, A_a initially decreases with time during stage 1, and its initial value is close to A (even though there are some holes on the film at the beginning of the experiments, for all practical purposes, we will consider $A_a/A = 1$ at that point).

If we consider that the aqueous solution in the system is perfectly mixed, a balance of abietic acid in the bulk solution gives

$$\frac{dN_A}{dt} = k_A A(C_A^* - C_A) \quad (2)$$

where N_A represents the moles of abietic acid removed from the disk ($N_A = C_A V$, where V is the total volume of aqueous solution).

On the other hand, r_A is controlled by the amount of abietic acid in the aqueous phase at the interface. We will assume that the adsorption rate of abietic acid is linear with abietic acid concentration, i.e., $r_A = kC_A^*$, where k is the rate constant for the process. Using this relationship and combining eqs 1 and 2 yields

$$\frac{dN_A}{dt} = k_A A \frac{r_R - kC_A}{k_A/\xi + k} \quad (3)$$

where $\xi = A_a/A$ represents the exposed film surface area expressed as a fraction of total disk area.

If N_A is expressed in terms of C_A, eq 3 is a first-order differential equation whose solution gives the abietic acid concentration in the surfactant solution as a function of time. The initial condition is the absence of abietic acid in the bulk solution ($C_A = 0$) at the start of the cleaning process ($t = 0$).

The right-hand side of eq 3 represents the cleaning rate during stage 1. At short times ($t \rightarrow 0$), the rate approaches a non-zero value. At longer times, a decrease in the surface area of organic phase (decrease in ξ) leads to lower cleaning rates. Furthermore, at longer times, C_A increases due to the progressive solubilization of abietic acid. Even though this increase is not significant, since abietic acid concentrations in solution are always relatively small, an increase in C_A also leads to a decrease in the cleaning rate due to the increase in adsorption rates.

To integrate eq 3, it is necessary to know how ξ varies with time. However, in most of the experiments, the cleaning curve during the first stage is a straight line, which indicates that a reduction of the stage 1 cleaning rate is precluded by the transition to the second state. For this reason, we have only quantified the initial cleaning rate in stage 1, given by taking the limit of eq 3 as $t \rightarrow 0$. If we assume that initially $\xi = 1$, we obtain

$$\left.\frac{dN_A}{dt}\right|_{t=0} = k_1 = \frac{k_A A r_R}{k_A + k} \quad (4)$$

The initial cleaning rate in stage 1 (k_1) is therefore a function of surfactant concentration (through r_R) and all the parameters that affect the mass-transfer coefficient and readsorption rate constant.

The disk rotating speed affects the initial cleaning rate through the mass-transfer coefficient, k_A. Under laminar flow conditions, there is a simple well-known relation expressing the dependence of mass-transfer coefficient on rotational rate (Levich, 1942),

$$k_A = 0.6205 \nu_2^{-1/6} D_A^{2/3} \omega^{1/2} \quad (5)$$

where ν_2 is the kinematic viscosity of the aqueous phase (which can be taken to be approximately equal to that of water) and D_A is the diffusion coefficient of the micelles that are transported from the surface to the bulk solution.

Equations 4 and 5 indicate that a plot of the inverse of the initial cleaning rate vs $\omega^{-1/2}$ should be a straight line with a slope directly proportional to k/r_R and an intercept equal to $(Ar_R)^{-1}$. Figure 7 shows such plots for the data gathered in this work at various surfactant concentrations. The lowest concentration (6×10^{-5} M) is below the cmc for the water−surfactant system, whereas the other two are above the cmc. The error bars correspond to average deviations obtained for each concentration by using a total of more than 10 repeated experiments over the whole range of rotational speeds. Notice that, even though there is a large degree of scatter for the low concentration data, the trends of the curves seem to follow the fitted straight lines. From the slope and intercept of these lines, we have calculated r_R and the parameter $k\omega^{1/2}/k_A$, whose dependence on surfactant concentration is solely due to changes in the

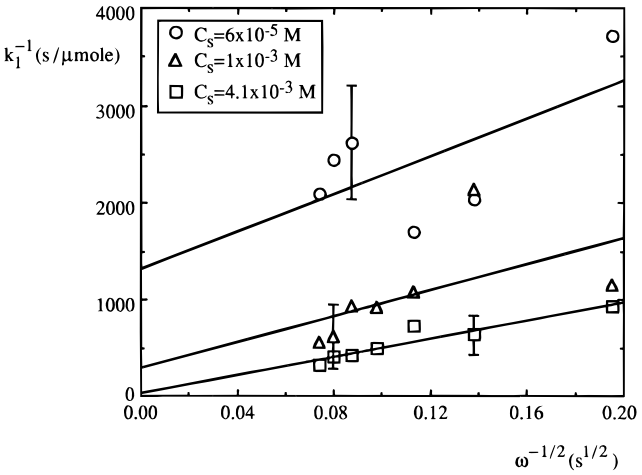

Figure 7. Scaling of stage 1 rates with rotational speed.

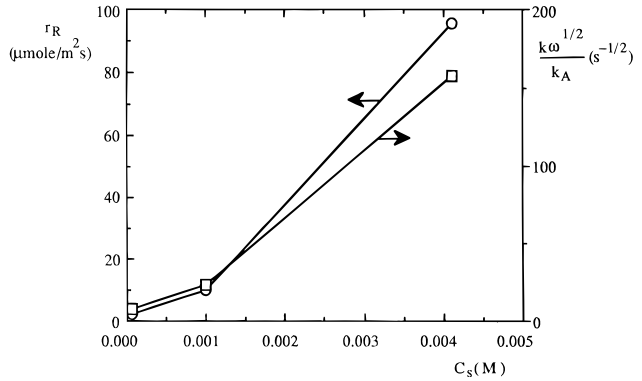

Figure 8. Dependence of stage 1 rates and readsorption coefficient on surfactant concentration.

adsorption rate constant k. The results are presented in Figure 8. This plot shows that both the specific rate of removal of abietic acid from the interface and the rate constant for the readsorption process increase with surfactant concentration following similar trends. Both parameters are related to the formation of abietic acid micelles, whose frequency and number increase as the surfactant concentration is increased. It is interesting to note that the values of those parameters for the lowest concentration (below the cmc) are relatively small, even though removal still exists. Note that the cmc concentration might be decreased by the presence of abietic acid.

In the results presented above, k and k_A are of the same order of magnitude so that both terms in the denominator of eq 4 are significant. It is interesting to note that, for very fast readsorption rates ($k \gg k_A$), the initial cleaning rate would be proportional to $\omega^{-1/2}$, whereas for slow readsorption rates ($k \ll k_A$), the initial cleaning rate would be independent of rotational speed.

Equation 4 indicates that the initial cleaning rate in stage 1 should be independent of initial film thickness. Preliminary information collected by Beaudoin et al. (1995a,b) indicates that first-stage rates for disks with three successive coatings are lower than those obtained with a single coating; i.e., the first-stage rate exhibits an apparent decrease with an increase in film thickness. This would seem to reflect a diffusion limitation not considered in the present analysis. However, we have visually determined that the film becomes smoother as additional coatings are applied. The roughness of the film when it has a single coating might account for an increased area for solubilization. The apparent decrease

of first-stage rates might therefore be due to a reduction in effective area. This aspect of the work is currently being investigated.

Transition between Stages 1 and 2. As the analysis of the photographs presented in the previous section shows, toward the end of stage 1, there is a swelling of the film on the disk, due to the partitioning of surfactant and water. This swelling process liquefies the film, which leads to the droplike structures observed in Figure 7a. The viscosity of the liquid in these drops is substantially lower than that of the original film, and hence, they start to move relative to the surface under the action of the shear stress exerted by the aqueous solution. This motion leads to drop coalescence and the formation of organic-phase rivulets which are the primary structures through which the abietic acid is removed from the disk during stage 2 (see below). This indicates that the necessary conditions for the onset of stage 2 are (a) a lowering of the organic-phase viscosity due to its takeup of surfactant and water, (b) the motion of organic-phase drops on the surface, and (c) the coalescence of these drops. The starting point for the occurrence of these conditions is the honeycomb structure that appears during the solubilization process in stage 1.

We have argued that surfactant partitioning into the film is a fast step (see Appendix). This means that the limiting factor in the swelling of the organic film is the rate of water partitioning. Since external transport processes are relatively fast (water is in excess), the controlling step must be the rate of water solubilization into the organic phase. If we denote by r_w the specific solubilization rate of water into the film, a mole balance of water within the film, neglecting internal diffusion limitations, would be

$$\frac{d(V_f C_{fw})}{dt} = r_w A_a \tag{6}$$

where V_f is the organic film volume and C_{fw} is the concentration of water within the film. The increase of C_{fw} with time leads to a reduction in film viscosity until a certain water concentration is reached, at which the viscosity is low enough that the drops of swollen film start to move on the surface under the action of the shear forces. The coalescence of these drops leads to the formation of rivulets and the onset of stage 2.

The experimental data indicate that the onset time for the transition to stage 2, t_c, is inversely proportional to the rotational speed, as evidenced by Figure 9. Best-fit straight lines have been drawn for comparison purposes. This scaling between t_c and ω is a consequence of the effect of rotational speed on temporal changes of the film geometry (which affect the changes in water concentration in the film, eq 6) and on the motion of drops on the surface. However, the interplay between viscosity and interfacial properties of the organic-phase drops with their motion on the surface and swelling rate is not completely clear.

The proportionality constant between t_c^{-1} and ω increases with surfactant concentration; i.e., when the surfactant concentration increases, the first stage is shorter. The cause for this behavior is most likely the increase in r_w with increases in surfactant concentration.

Beaudoin et al. (1995a) reported that an increase in the initial film thickness leads to an increase in the onset time for stage 2. This trend is consistent with the mechanism proposed above, since a thicker initial film implies a larger initial value of V_f, and this leads to a lower rate of increase of water concentration in the film, at a given solubilization rate (in essence, the more material the film contains initially, the more water it would have to absorb to liquefy, which would take longer).

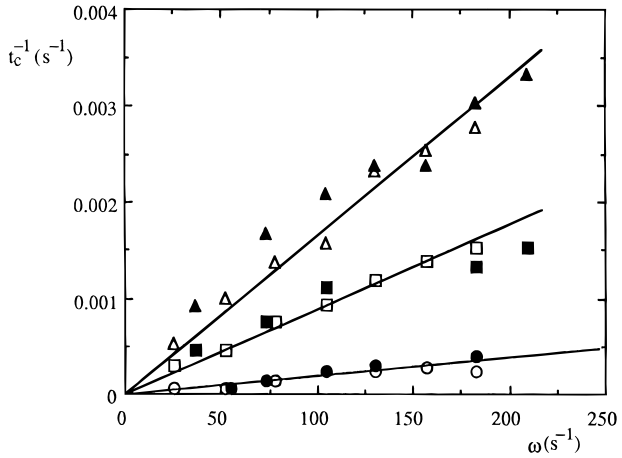

Figure 9. Scaling of stage 2 onset times with rotational speeds; circles, $C_s = 6 \times 10^{-5}$ M; squares, $C_s = 1 \times 10^{-3}$ M; triangles, $C_s = 4.1 \times 10^{-3}$ M. Open symbols, this work; filled symbols, Beaudoin et al. (1995a).

Stage 2. During this stage, the observations made indicate that the cleaning process is controlled by the hydrodynamics of the motion induced by the rotation of the disk in the stagnant aqueous solution. In this section, we will show why the preferred structures for aggregation of the organic-phase drops are in the shape of spiral rivulets. Afterwards, we will develop a model to simulate the cleaning process during this stage.

In order to analyze the hydrodynamics of the process, we will start by considering the motion of the aqueous solution induced by the rotation of the disk. If we take into account that the film is stagnant or moving at low speeds relative to the disk and neglect the effect of irregularities on the film surface, we can assume that the motion of the water is approximately that induced by a smooth disk rotating at a constant speed ω. The solution to the Navier−Stokes equations for this case is well-known (Schlichting, 1968). These equations admit a similarity solution in terms of the following variables;

$$\xi = z\left(\frac{\omega}{\nu_2}\right)^{1/2} \tag{7}$$

$$v_{r2} = \omega r f_2(\xi) \tag{8}$$

$$v_{\theta 2} = \omega r g_2(\xi) \tag{9}$$

$$v_{z2} = (\omega \nu_2)^{1/2} h_2(\xi) \tag{10}$$

$$P = \mu_2 \omega p_2(\xi) \tag{11}$$

where the subindex 2 refers to the aqueous phase (see Figure 10 for notation), v_r, v_θ, and v_z are the components of the velocity vector, P is the modified pressure (including gravitational contributions), ξ is a similarity variable, and f_2, g_2, h_2, and p_2 are similarity functions that

satisfy the following set of ordinary differential equations and boundary conditions:

$$h_2' + 2f_2 = 0 \tag{12}$$

$$f_2^2 - g_2^2 + h_2 f_2' - f_2'' = 0 \tag{13}$$

$$2f_2 g_2 + h_2 g_2' - g_2'' = 0 \tag{14}$$

$$h_2 h_2' + p_2' - h_2'' = 0 \tag{15}$$

$$\xi = 0: \qquad g_2 = 1, \quad f_2 = h_2 = 0, \quad p_2 = 0 \tag{16}$$

$$\xi \to \infty: \qquad f_2 = g_2 = 0 \tag{17}$$

where the primes denote derivative with respect to ξ. This set of equations can be solved numerically. The solution is reported by Schlichting (1968).

The above system of equations provides the velocity and pressure fields of the aqueous solution. From this, it is possible to calculate the stress vector that the aqueous solution exerts on the surface of the disk, $\mathbf{t}_s$, which can be shown to include solely contributions from the viscous stress tensor, $\boldsymbol{\tau}$,

$$\mathbf{t}_s = \tau_{zr}|_{z=0}\mathbf{e}_r + \tau_{z\theta}|_{z=0}\mathbf{e}_\theta \tag{18}$$

Here $\mathbf{e}_r$ and $\mathbf{e}_\theta$ are unit vectors in the radial and angular direction, respectively. Expressing the components of the viscous stress tensor in terms of velocity gradients and using the similarity variables defined above leads to

$$\mathbf{t}_s = [f_2'(0)\mathbf{e}_r + g_2'(0)\mathbf{e}_\theta](\mu_2\rho_2)^{1/2} r\omega^{3/2} \tag{19}$$

where $f_2'(0) = 0.510$ and $g_2'(0) = -0.616$. This equation shows that each of the components of the stress vector is directly proportional to the radial position.

During stage 2, the motion of the aqueous solution controls the behavior of the organic film on the surface of the disk. At this point, the film has been liquefied into drops. The stress vector given by eq 19 acts on the drops at each point in the disk. It is reasonable to think that, on the average, the drop motion on the surface will tend to follow the direction of the stress vector so that, after coalescence, drop aggregation should follow lines tangent to $\mathbf{t}_s$ at each point (which we will term stress lines). The shape of the stress lines can be evaluated from eq 19. Let $\boldsymbol{\lambda}$ be a unit vector tangent to the stress line at every point. Then, according to the definition of stress line, we have

$$\mathbf{t}_s = t_s\boldsymbol{\lambda} \tag{20}$$

The stress line is then described by a position vector $\mathbf{r}(s)$, where s is the arc length along the line, and

$$\boldsymbol{\lambda} = \frac{d\mathbf{r}}{ds} \tag{21}$$

In cylindrical coordinates on the surface of the disk, the stress line can be described as $r_s = r_s(\theta)$, where r_s represents the radial coordinate of a point in the line. From eq 21, we obtain

$$\frac{1}{r_s}\frac{dr_s}{d\theta} = \frac{\lambda_r}{\lambda_\theta} \tag{22}$$

By using eqs 19 and 20, this leads to

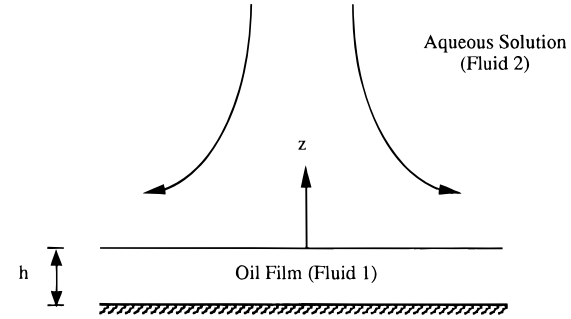

Figure 10. Diagram of film on the rotating disk.

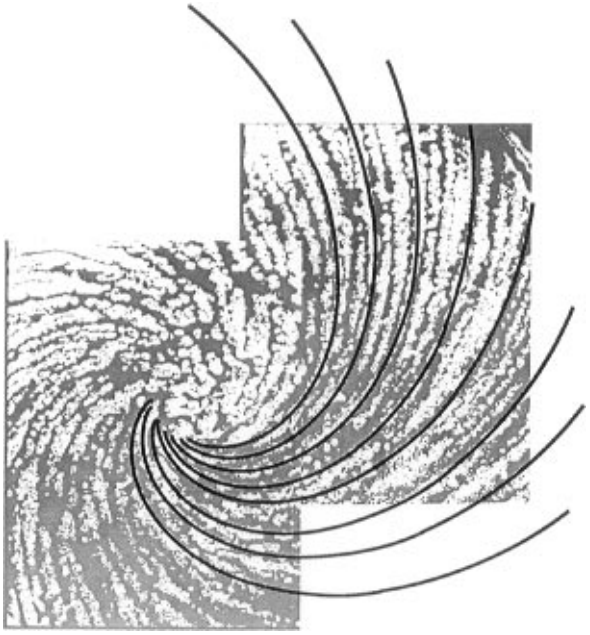

Figure 11. Comparison between stress lines generated from eq 22 and experimental film morphology from Figure 6b. Organic film appears dark; laminate surface is white.

$$\frac{1}{r_s}\frac{dr_s}{d\theta} = \frac{f_2'(0)}{g_2'(0)} = -0.8279 \tag{23}$$

Upon integration, this equation yields

$$r_s = r_0 e^{-0.8279\theta} \tag{24}$$

According to the above discussion, eq 24 should represent the shape of the rivulets observed during stage 2 (see Figures 5 and 6). Figure 11 shows the superposition of lines generated by eq 24 on a digitized composite of takes 1 and 2 in Figure 6b. Notice that the organic-phase rivulets follow the stress lines, except for some minor irregularities and deviations caused by possible instabilities in the creation and surface motion of the contact lines.

The fact that the magnitude of the stress vector is larger toward the edge of the disk explains why the formation of the organic-phase rivulets starts there and then progresses to the center, as can be gathered from the sequence shown in Figure 5. The fact that the stress tends to zero at the center also explains why the rivulets tend to disappear at the central region of the disk, where the organic phase remains in isolated drops: there is not enough force there to cause drop motion and aggregation.

After the rivulets are formed under the action of the shear stress, each of them can be conceived as a film of

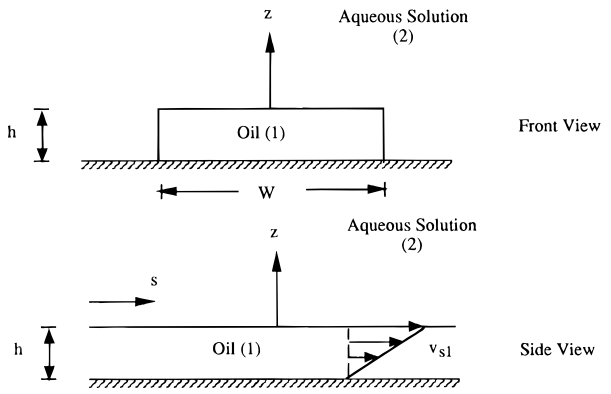

Figure 12. Shape of rivulets used in the theoretical analysis.

organic phase with relatively low viscosity, upon which a shear force is acting. This shear force has a direction parallel to the film at each point, and its points toward the edge of the disk. This force causes the organic phase to move toward the edge and eventually come off the disk.

Summarizing, the cleaning of the disk during stage 2 consists in the removal of abietic acid through the edges due to the action of the shear stress exerted by the relative motion of the aqueous solution. This means that the second stage of cleaning is controlled by the hydrodynamics of the process and not by diffusion and interface processes, as was the case for stage 1. Beaudoin et al. (1995b) reached this general conclusion based on an empirical analysis of the effect of several experimental variables on cleaning rates. In this work, we have confirmed this conclusion and established the precise nature of the removal mechanism.

It is interesting to point out that it is possible to show that the centripetal acceleration of the organic phase due to the rotational motion of the disk is negligible when compared to the forces given by eq 19 for the conditions employed in the present work. This indicates that the removal of organic phase through the edges is not a simple spin-off process.

The study of the thinning of a rivulet of organic phase due to an external shear stress can be used as a preliminary model to represent the cleaning process during stage 2. We will consider the following simplified conceptualization. First, we invoke the observation that the rivulet thickness in the disk plane is small with respect to its length to assume that we can visualize the rivulet as a rectilinear film of liquid, thus neglecting its curvature. In addition, since centripetal forces are negligible, we can consider that the rivulet is fixed at the bottom and perceives a force at the top given by eq 19. For simplification purposes, we will assume this film to have a rectangular cross section of thickness h, as shown in Figure 12. It is necessary to point out that the shape of the cross section will not have an impact on the qualitative conclusions that will be gathered with this analysis.

Let s be a spatial coordinate along the rivulet, $0 \leq s \leq L$, where L is the total length of the rivulet, which can be calculated from eq 24 to be $L = 1.568R$, where R is the disk radius. In the new coordinate system, the stress vector $\mathbf{t}_s$ is a force per unit area in the s direction. This force should equal the $z-s$ component of the viscous stress tensor acting on the organic phase within the rivulet. This viscous stress is a function of s through the dependence of $\mathbf{t}_s$ on r. However, its dependence on s can be considered to be relatively weak (lubrication approximation) since the length of the rivulet is much larger than its thickness. At each point in s, the action of this force then generates a linear velocity profile given by

$$v_{s1} = \frac{0.510(\mu_2\rho_2)^{1/2}\omega^{3/2}}{\mu_1}(h + z)s \tag{25}$$

where μ_1 is the viscosity of the liquid in the film.

If we assume that the film thickness (h) is uniform along the rivulet, the use of the continuity equation leads to

$$\frac{\mathrm{d}h}{\mathrm{d}t} + \frac{1}{W}\frac{\mathrm{d}q}{\mathrm{d}s} = 0 \tag{26}$$

where W is the width of the rivulet (see Figure 12) which is assumed to be constant and q is the flow rate of organic phase that flows through the cross section at position s,

$$q = W\int_{-h}^{0} v_{s1}\,\mathrm{d}z \tag{27}$$

Substituting eq 25 into eq 27 and combining the result with eq 26 leads to

$$\frac{\mathrm{d}h}{\mathrm{d}t} + \frac{0.255(\mu_2\rho_2)^{1/2}\omega^{3/2}}{\mu_1}h^2 = 0 \tag{28}$$

This equation is similar to that obtained by Middleman (1987) for the thinning of a uniform film of liquid on a rotating disk. The equation can be integrated to obtain how the thickness of the rivulet changes with time. The result is

$$\frac{1}{h} = \frac{1}{h_0} + \frac{0.255(\mu_2\rho_2)^{1/2}\omega^{3/2}}{\mu_1}(t - t_c) \tag{29}$$

where h_0 is the initial rivulet thickness, which occurs at the beginning of the second stage ($t = t_c$).

The rate at which organic phase is cleaned from the disk can be related to the rate of thinning of the rivulets by means of a mole balance,

$$\frac{\mathrm{d}N_A}{\mathrm{d}t} = -\frac{n_R WL\rho_1}{M}\frac{\mathrm{d}h}{\mathrm{d}t} \tag{30}$$

where M is the molecular weight of the abietic acid and n_R is the number of rivulets (we are implicitly assuming all the rivulets to be of the same geometry). The removal rate decreases with time by virtue of the decrease of h. However, in the real process, the cleaning rate is expected to decrease more abruptly with time since the rivulets start to break at some point, as evidenced by the photographic analysis presented earlier. This implies that eq 30 should only be applicable to the beginning of stage 2. From the experimental cleaning curves, we can obtain the cleaning rate at precisely the beginning of stage 2 ($t = t_c$). According to our model, this rate should be given by substituting eq 28 into eq 30 and taking $h = h_0$. The result is

$$\left(\frac{\mathrm{d}N_A}{\mathrm{d}t}\right)_{t=t_c(\text{stage 2})} = k_2 = \frac{n_R WL\rho_1}{M}\frac{0.255(\mu_2\rho_2)^{1/2}\omega^{3/2}}{\mu_1}h_0^{\,2} \tag{31}$$

Equation 31 indicates that the initial removal rate in stage 2 should be directly proportional to $\omega^{3/2}$,

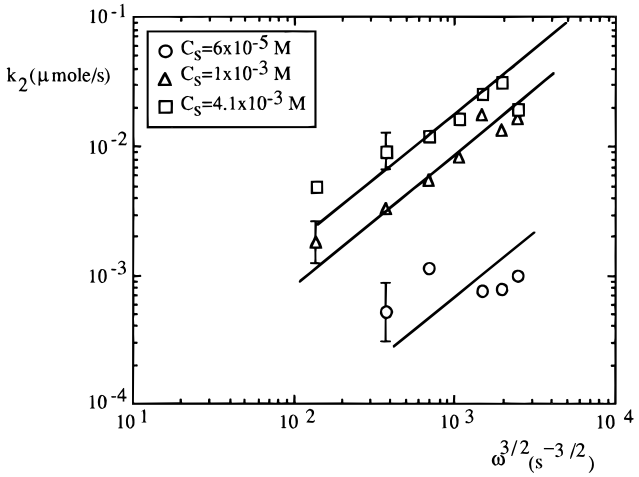

Figure 13. Scaling of stage 2 rates with rotational speed.

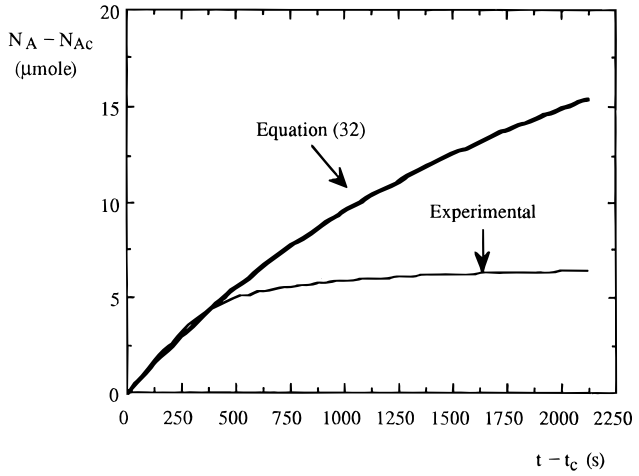

Figure 14. Comparison between rivulet draining model and experimental data for stages 2 and 3. The experiment corresponds to a surfactant concentration of 1×10^{-3} M and a rotational speed of 1500 rpm.

providing that the factor that groups rivulet frequency and geometry does not change appreciably with rotational speed. Notice that this dependence is a direct consequence of the functional relationship between the shear stress and rotational speed, as expressed by eq 19. The effect of rotational speed on stage 2 rates was analyzed by Beaudoin et al. (1995b), who found the $\omega^{3/2}$ dependence from an analysis of experimental data. This dependence is verified in Figure 13, where we have plotted initial rates during the second stage obtained as the slopes of the experimental cleaning curves during the second stage at the onset. Solid lines in this plot are lines with unit slope that have been drawn for comparison purposes. Notice that, despite the scatter, the data seem to follow the predicted trend, especially at high surfactant concentrations and rotational speeds.

There is also a noticeable effect of surfactant concentration on second-stage cleaning rates. According to eq 31, the effect of surfactant concentration would be reflected in the physical properties of the film, mainly the film viscosity, μ_1. Presumably, as the concentration of surfactant increases, the film absorbs more water and its viscosity decreases, leading, according to eq 31, to an increased removal rate.

Beaudoin et al. (1995a) reported that the initial thickness of the film on the disk has no appreciable effect on k_2. The initial thickness was changed from that corresponding to one coating to a three-coating layer. Equation 31 predicts that the removal rate in the second stage depends on the initial thickness of the rivulets, h_0. In fact, it depends on the product of h_0 and the total volume of organic phase at t_c ($n_R WLh_0$). However, as discussed above, the value of t_c increases considerably for thicker films. This gives time for the solubilization process to remove more abietic acid from the film. This indicates that h_0 is not simply proportional to the initial thickness, and there seems to be a compensating effect between initial film thickness and time for stage 2 onset that leads to similar rates. This aspect of the process needs to be investigated further.

We have also explored to what extent the proposed model can be used to represent stage 2 data. For this purpose, we can integrate eq 30 and then use eq 29 to obtain how the moles removed in stage 2 vary with time. Starting from the fact that the initial slope (k_2) can be determined from the experimental data, we express the final equation in terms of this slope, which yields

$$N_A - N_{Ac} = \frac{k_2(t - t_c)}{1 + \frac{M}{n_R WL\rho_1 h_0} k_2(t - t_c)} \qquad (32)$$

where N_{Ac} is the amount of moles removed at $t = t_c$. From the experimental data, the slope of the cleaning curve at the beginning of stage 2 yields k_2, as indicated in eq 31. With this value known, this equation can be used to fit stage 2 data with one additional adjustable parameter, namely, the factor that multiplies the rate and time difference in the denominator. The fit of the data is not straightforward, since eq 32 loses its validity when the rivulets start to break and stage 3 begins. We fit eq 32 to the data at early times during stage 2. Figure 14 shows one such fit. It can be seen that around $t - t_c = 280$ s, eq 32 starts overpredicting the data. This may be the point at which the rivulet structure changes, leading to stage 3.

Equation 31 indicates that the organic-phase viscosity (μ_1) plays an important role in the cleaning rate for stage 2, which is, in this case, the stage in which cleaning proceeds faster. It would be valuable to have knowledge on the evolution of water content in the organic phase and how this affects the viscosity of the film. This line of investigation is being pursued by our research group. We have independently determined the viscosity of the organic phase at the start of the experiment by means of a rotational viscometer (Rheometrics stress rheometer). The film at that point consists of 75% abietic acid and 25% isopropyl alcohol. At 24 °C, this value is $\mu_1 =$ 3.8 Pa s. The value of μ_1 during stage 2 should be lower than this. We can use this value, along with eq 31, to estimate the order of magnitude of a lower bound for k_2. For this purpose, we have used the following values, indicative only of orders of magnitude: $n_R = 50$, $L =$ 0.01 m, $W = 0.001$ m, $h_0 = 10\ \mu$m. At $\omega = 1500$ rpm, eq 31 yields $k_2 = O(10^{-13}$ kmol/s), which is consistent with the results shown in Figure 13. This is an indication of the validity of eq 31.

Stage 3. The final portion of the cleaning curve exhibits removal rates that progressively decrease, since the moles removed approach asymptotically the total amount of abietic acid originally present in the disk. In this stage, the organic phase is distributed in the form of isolated drops on the surface. Some of these drops maintain part of the original spiral shape of the rivulets. During this stage, the continuing swelling of the organic film leads to a roll-up mechanism by which drops of

organic phase are detached from the surface under the action of shear forces. The analysis of this stage was performed in detail by Beaudoin et al. (1995b). The rate of removal of abietic acid is assumed to be proportional to the amount of acid remaining on the disk in the form of isolated drops. The solution leads to an exponential decay of the removal rate as the disk surface approaches a clean surface.

Conclusions

We have examined the mechanisms responsible for the removal of abietic acid films from a rotating disk immersed in a solution of a nonionic surfactant. The results show how different factors affect the cleaning mechanisms at different stages of the process. For the system studied in this work, the cleaning starts with a solubilization mechanism (stage 1) in which mass transfer plays an important role. Subsequently, a second stage controlled by hydrodynamic forces sets in. In this stage, the organic phase is organized into liquid structures (rivulets) and the removal occurs at the edges of the disk. The rivulets follow lines tangent to the stress exerted by the water on the surface of the organic phase. As the organic phase on the surface is depleted, the final stage consists of roll up in which hydrodynamics is once again the controlling phenomenon. The results presented in this work show that the removal of organic films from surfaces is a complex process in which the controlling factors depend not only on the operating conditions but also on the evolution of the process itself. It is interesting to point out that the process described here is not necessarily the same for all other experimental conditions. For instance, it is possible to conceive a film that never liquefies and is cleaned by pure solubilization. However, the conditions explored in this work seem to present the most complex situation that can be encountered in this type of cleaning process.

Acknowledgment

This work was funded by the National Science Foundation Program for Environmentally Benign Chemical Synthesis and Processing (Grant No. CTS-9216850). Northern Telecom Co. in Research Triangle Park, NC, provided the FR-4 laminate. We acknowledge the laboratory assistance of Percy McIntyre and the help provided by Inge Simonsen on photographic techniques. Useful discussions with Steve Beaudoin and Stephanie Tolstedt-Read are also greatly appreciated.

Appendix. Surfactant Mass Transfer and Diffusion

In the analysis of the solubilization process during stage 1, we have assumed that the transport of surfactant to the water−organic phase interface is fast with respect to a characteristic time of the cleaning process during that stage. In addition, we have considered surfactant adsorption and partitioning into the film to be fast.

First of all, we can estimate a characteristic time for the process of surfactant diffusion within the organic film, t_D, by

$$t_D \approx \frac{h^2}{D_s} \tag{A.1}$$

where D_s is the diffusion coefficient of $C_{12}E_5$ in the abietic acid film. The diffusion coefficient of this surfactant in water has been estimated to be 4×10^{-10} m^2/s (Beaudoin et al., 1995b). We will assume $D_s = O(10^{-10}$ m^2/s) and h to be equal to the initial film thickness ($h = 10^{-7}$ m), which leads to $t_D \approx 10^{-4}$ s. This value is negligible compared to the characteristic times of stage 1, which are of the order of minutes. Notice that a diffusion coefficient several orders of magnitude lower than that assumed would still make the diffusion process very fast.

To study the mass transfer of surfactant from the bulk solution to the film, and in agreement with the preceding analysis, we will consider that diffusion within the film is fast so that we can consider the film to have a uniform surfactant concentration. In this case, if we assume that adsorption and desorption of surfactant at the interface are also fast processes, a mass balance of surfactant in the film, assuming that it completely covers the disk, is described by the differential equation

$$\frac{dC_{sf}}{dt} = \frac{k_m}{h}\left(C_s - \frac{C_{sf}}{K}\right) \tag{A.2}$$

where C_{sf} is the concentration of surfactant in the film, k_m is the mass-transfer coefficient of surfactant from the bulk aqueous solution to the interface, and K is the equilibrium constant that governs the partitioning of surfactant between aqueous and organic phases.

The solution of the differential equation (A.2) leads to the result

$$C_{sf} = KC_s(1 - e^{-[k_m/(hK)]t}) \tag{A.3}$$

From this equation, it can be seen that a characteristic time for the mass-transfer process is

$$t_m = \frac{hK}{k_m} \tag{A.4}$$

The mass-transfer coefficient can be evaluated from

$$k_m = 0.6205\nu_2^{-1/6}D^{2/3}\omega^{1/2} \tag{A.5}$$

where $D = 4 \times 10^{-10}$ m^2/s and $K = 6500$ (Beaudoin et al., 1995a). Using the lowest rotational speed employed in this work (250 rpm), we obtain $t_m = 38$ s, which is small compared to stage 1 times for that rotational speed.

The analysis performed above indicates that in the characteristic times that stage 1 spans in the cleaning process, the transport of surfactant from the bulk of the aqueous solution to the interface and its subsequent penetration into the organic film can be considered as instantaneous.

Literature Cited

Beaudoin, S. P. Mechanisms of Removal of Organic Films from Solid Surfaces Using Aqueous Solutions of a Nonionic Surfactant. Ph.D. Dissertation, North Carolina State University, Raleigh, 1995.

Beaudoin, S. P.; Grant, C. S.; Carbonell, R. G. Removal of Organic Films from Solid Surfaces Using Aqueous Solutions of Nonionic Surfactants. 1. Experiments. *Ind. Eng. Chem. Res.* **1995a**, *34*, 3307.

Beaudoin, S. P.; Grant, C. S.; Carbonell, R. G. Removal of Organic Films from Solid Surfaces Using Aqueous Solutions of Nonionic Surfactants. 2. Theory. *Ind. Eng. Chem. Res.* **1995b**, *34*, 3318.

Levich, B. The Theory of Concentration Polarization. *Acta Phisicochim. URSS* **1942**, *17*, 257.
Middleman, S. The Effect of Induced Air-Flow on the Spin Coating of Viscous Liquids. *J. Appl. Phys.* **1987**, *62*, 2530.
Miller, C. A.; Raney, K. H. Solubilization-Emulsification Mechanisms of Detergency. *Colloids Surf. A* **1993**, *74*, 169.
Rosen, M. J. *Surfactants and Interfacial Phenomena*; John Wiley and Sons: New York, 1989.
Shaeiwitz, J. A.; Chan, A. F.-C.; Cussler, E. L.; Evans, D. F. The Mechanism of Solubilization in Detergent Solutions. *J. Colloid Interface Sci.* **1981**, *84*, 47.
Schlichting, H. *Boundary Layer Theory*, 6th ed.; McGraw-Hill: New York, 1968.
Thomas, S.; Faghri, A.; Hankey, W. Experimental Analysis and Flow Visualization of a Thin Liquid Film on a Stationary and Rotating Disk. *J. Fluids Eng.* **1991**, *113*, 73.

Received for review April 8, 1996
Revised manuscript received August 14, 1996
Accepted August 20, 1996[⊗]

IE960195C

[⊗] Abstract published in *Advance ACS Abstracts,* October 15, 1996.